Special Issue

The Pattern of Visual Fixation Eccentricity and Instability in Optic Neuropathy and Its Spatial Relationship to Retinal Ganglion Cell Layer Thickness

Robert M. Mallery,[1–3] Pieter Poolman,[4] Matthew J. Thurtell,[3,4] Jui-Kai Wang,[4,5] Mona K. Garvin,[4,5] Johannes Ledolter,[4] and Randy H. Kardon[3,4]

[1]Department of Neurology, Brigham and Women's Hospital, Boston, Massachusetts, United States
[2]Department of Ophthalmology, Massachusetts Eye and Ear Infirmary, Boston, Massachusetts, United States
[3]Department of Ophthalmology and Visual Sciences, University of Iowa Hospitals and Clinics, Iowa City, Iowa, United States
[4]Iowa City VA Center for the Prevention and Treatment of Visual Loss, Iowa City, Iowa, United States
[5]Department of Electrical and Computer Engineering, University of Iowa, Iowa City, Iowa, United States

Correspondence: Robert M. Mallery, Department of Neurology, Brigham and Women's Hospital, 75 Francis Street, Boston, MA 02115, USA; robert_mallery@meei.harvard.edu.

Submitted: December 14, 2015
Accepted: April 7, 2016

Citation: Mallery RM, Poolman P, Thurtell MJ, et al. The pattern of visual fixation eccentricity and instability in optic neuropathy and its spatial relationship to retinal ganglion cell layer thickness. *Invest Ophthalmol Vis Sci*. 2016;57:OCT429–OCT437. DOI:10.1167/iovs.15-18916

Purpose. The purpose of this study was to assess whether clinically useful measures of fixation instability and eccentricity can be derived from retinal tracking data obtained during optical coherence tomography (OCT) in patients with optic neuropathy (ON) and to develop a method for relating fixation to the retinal ganglion cell complex (GCC) thickness.

Methods. Twenty-nine patients with ON underwent macular volume OCT with 30 seconds of confocal scanning laser ophthalmoscope (cSLO)-based eye tracking during fixation. Kernel density estimation quantified fixation instability and fixation eccentricity from the distribution of fixation points on the retina. Preferred ganglion cell layer loci (PGCL) and their relationship to the GCC thickness map were derived, accounting for radial displacement of retinal ganglion cell soma from their corresponding cones.

Results. Fixation instability was increased in ON eyes (0.21 deg^2) compared with normal eyes (0.06982 deg^2; $P < 0.001$), and fixation eccentricity was increased in ON eyes (0.48°) compared with normal eyes (0.24°; $P = 0.03$). Fixation instability and eccentricity each correlated moderately with logMAR acuity and were highly predictive of central visual field loss. Twenty-six of 35 ON eyes had PGCL skewed toward local maxima of the GCC thickness map. Patients with bilateral dense central scotomas had PGCL in homonymous retinal locations with respect to the fovea.

Conclusions. Fixation instability and eccentricity measures obtained during cSLO-OCT assess the function of perifoveal retinal elements and predict central visual field loss in patients with ON. A model relating fixation to the GCC thickness map offers a method to assess the structure–function relationship between fixation and areas of preserved GCC in patients with ON.

Keywords: fixation, OCT, optic neuropathy, ganglion cell

Fixational eye movements function to stabilize images on the retina and are a major target for rehabilitation strategies for visual loss due to macular scotomas. Abnormalities of fixation are well described in patients with macular scotomas due to retinal disease and geographic atrophy, for which the precise retinal loci of fixation can be related to the region of geographic atrophy using confocal scanning laser ophthalmoscope (cSLO)-based technology. When macular disease affects the fovea, patients frequently adopt an alternate preferred retinal locus (PRL) of fixation eccentric to the fovea.[1–3] The PRL and the stability of fixation influence visual acuity obtained and performance on visually demanding tasks such as reading.[4,5] Improvement in visual acuity has been shown to mirror improvement in fixation stability in patients with AMD treated with intravitreal anti–vascular endothelial growth factor (VEGF) therapy,[6] and rehabilitative strategies targeted on modifying fixation and improving reading speed have been proposed as a major form of therapy in patients with low vision.

Less is known about how fixation is altered by optic neuropathies (ONs) that involve central vision. Fixation abnormalities in patients with ON are becoming increasingly recognized, and similar diagnostic and rehabilitative strategies may be applicable for patients with central vision loss related to ON.[7–10] In ON, the spatial pattern of neuron loss across the macula may influence the PRL, but a method to compare fixation loci with the thickness of the inner retina layers has been lacking. In contrast to macular degeneration, cSLO images of the retina may appear normal in ON. Spatial correlation of the distribution of fixation loci on the retina with the corresponding retinal ganglion cell layer (GCL) thickness may provide new insights into the fixation pattern of a patient with ON.

Confocal SLO–optical coherence tomography (cSLO-OCT) offers a promising means for assessing fixation abnormalities in patients with ON. For example, during a Spectralis OCT examination (Heidelberg Engineering, Heidelberg, Germany), a

Investigative Ophthalmology & Visual Science

patient is asked to fixate on a target while a cSLO tracks retinal position during the acquisition of the OCT scan. By saving the retinal positions during the OCT scan, a high-resolution record of fixation is available from the device. Segmentation of the OCT volume scan also allows fixation data from the cSLO to be related to the structural integrity of individual retinal layers. Here we introduce a method that utilizes the eye tracking coordinates recorded during OCT acquisition to localize fixation points on the retina, derive measures of fixation, and relate fixation to the thickness of the ganglion cell complex (GCC), which is a combination of the GCL and inner plexiform layer (IPL). We assessed whether measures of fixation can identify eyes with ON and central scotomas, and we characterized the topographic relationship between the fixation pattern on the retina and the GCC in eyes with unilateral and bilateral ON.

Methods

Subjects

Twenty-nine patients with ON (20 unilateral and 9 bilateral) were recruited prospectively from the neuro-ophthalmology clinic at the University of Iowa Department of Ophthalmology and Visual Sciences. After exclusion of eyes with concurrent retinal abnormalities, the two study groups consisted of 35 eyes with ON and 19 unaffected eyes. Mean subject age was 51 years, and the etiology and duration of ON varied among patients, including nonarteritic ischemic ON (NAION; $n = 7$; duration [years]: 0.08, 0.3, 0.6, 0.83, 1.8, 3.1, 12.6), arteritic ION ($n = 3$; duration [years]: 1.3, 2.2, 5.0), nonarteritic posterior ION ($n = 2$; duration [years]: 1.3, 3.1), compressive ON ($n = 7$; duration [years]: 0.6, 1.8, 2.6, 2.8, 2.8, 6.6, 22), demyelinating optic neuritis ($n = 6$; duration [years]: 0.08, 0.08, 0.1, 1.0, 6.0, 6.9), Leber hereditary ON ($n = 2$; duration [years]: 0.3, 3.6), optic disc drusen ($n = 1$; duration [years]: 0.12), and optic nerve hypoplasia ($n = 1$; congenital). Of the six patients with optic neuritis, three (two with central scotomata) were evaluated within 6 weeks of developing vision loss, and three (two with persistent central scotomata) were evaluated after more than 1 year. Snellen visual acuity and perimetry were performed on all patients. Visual fields were assessed using either Goldmann kinetic perimetry (26 patients) or automated perimetry (3 patients) with a Humphrey Field Analyzer II (Carl Zeiss Meditec, Inc., Jena, Germany) and the 24-2 Swedish Interactive Thresholding Algorithm (SITA) standard protocol.

The research adhered to the tenets of the Declaration of Helsinki, and the research was approved by the institutional review board at the University of Iowa. Written, informed consent was obtained from the subjects after explanation of the nature and possible consequences of the study.

Optical Coherence Tomography With Retinal Tracking

Each patient underwent a macular volume cSLO-OCT using the Spectralis platform (Heidelberg Engineering). Each macular volume scan consisted of 49 vertically oriented B-scans spanning a 20° × 20° area. The SLO images and OCT B-scans were obtained at the high-resolution (HR) setting; the SLO resolution measured 1536 × 1536 pixels, and each B-scan measured 1024 × 496 pixels and consisted of a mean of nine individual B-scans registered by Heidelberg's Automatic Real-time Tracking (ART) system.

A program installed by Heidelberg Engineering logged the retinal position acquired during eye tracking at a frequency of 4.8 Hz, the frame rate for HR video on the Spectralis. This frame rate is based on the line scan speed of the SLO (8000 lines/s) and the time equivalent required to reset the scanning laser for the next frame (125 lines). Each row of the tracking log contained values representing an affine transformation of the reference SLO image of the OCT to the active SLO video frame, providing horizontal, vertical, and rotational values for eye position recorded at the 4.8-Hz frame rate. With the contralateral eye occluded, each patient was instructed to fixate on the central internal blue fixation target while eye tracking was logged for 30 seconds before acquisition of the OCT B-scans.

Localization of the Fovea and Retinal Fixation Points

Three-dimensional (3D) segmentation (Iowa Reference Algorithm) was applied to each macular volume scan to segment 10 retinal layers. The Iowa Reference Algorithm (http://www.biomed-imaging.uiowa.edu/downloads) is a fully 3D, automated algorithm,[11–14] which can accurately measure the macular GCL-IPL complex in the presence of optic disc edema. The incorporation of 3D information allows the Iowa Reference Algorithm to decrease segmentation error.[11–13] The boundaries of the macular GCL-IPL were defined by the junction between the retinal nerve fiber and ganglion cell layers and the junction between the inner plexiform and inner nuclear layers. The automated segmented layers were inspected for errors and manually corrected if present. The position of the fovea in the reference SLO image was identified as the thinnest portion of the retina between the internal limiting membrane and basement membrane (ILM-BM) within the foveola zone and manually corrected if necessary using the vertical B-scans and horizontal B-scan reconstructions (Figs. 1A–C). The initial point of fixation on the retina was the center of the reference image, which corresponds to both the optical center of the SLO and the location of the center fixation LED of the Spectralis. The full set of fixation points on the retina was derived by applying the affine transformation of the tracking log to the location of the initial fixation point (Fig. 1D).

Calculation of Fixation Instability, Preferred Retinal Loci, and Eccentricity

Kernel density estimation (KDE), a nonparametric method, was used to calculate the probability of fixating at each point on the retina with respect to the fovea. By a previously described method,[15] fixation instability for each eye was calculated as the area of the 68% isoline of the KDE (Fig. 1E). The PRLs were defined as the centroid of distinct retinal areas enclosed by a component of the 68% isoline and containing at least 10% of the total number for fixation points. Fixation eccentricity was defined as the weighted displacement of all PRL from the fovea (Fig. 2).

Comparative Measures of Visual Function

Snellen visual acuity was converted to log of the minimum angle of resolution (logMAR) by calculating the base 10 logarithm of 1 divided by the Snellen fraction. Kinetic Goldmann perimetry was objectively quantified by calculating visual field volume scores using only the I1e, I2e, and I4e isopters that were routinely assessed in all patients. The visual fields were scanned at high resolution, and ImageJ software (http://rsbweb.nih.gov/ij; provided in the public domain by the National Institutes of Health, Bethesda, MD, USA) and a touchscreen device were used to trace and calculate the area of each isopter minus any scotomata. To account for different image resolutions, the areas were normalized by the area enclosed by the central 60° of the

Investigative Ophthalmology & Visual Science

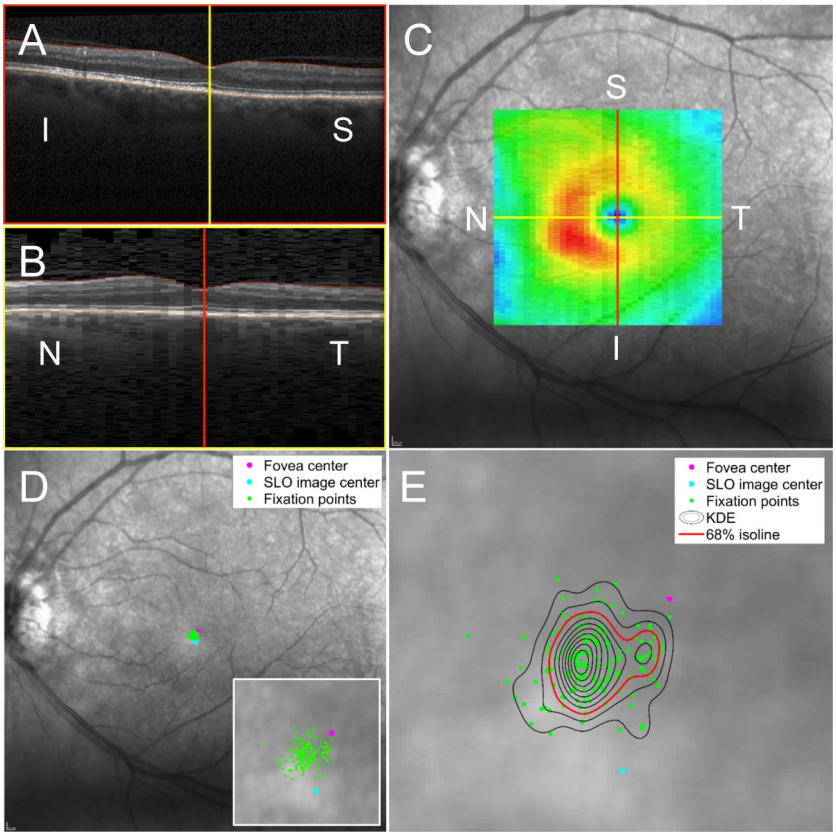

Figure 1. Localization of fixation points on the retina and the use of KDE to calculate the PRL and fixation instability**. (A**, **B**) Vertical OCT B-scans and horizontal B-scan reconstructions confirmed the location of the fovea center. (**C**) The retinal thickness map (ILM-BM) is shown overlying the SLO reference image used by the Spectralis ART tracking software. The foveal center is indicated by the intersection of the vertical and horizontal lines and is depicted on the thickness map as the central blue pixel area. (**D**) Fixation points on the retina are calculated by applying the retinal tracking coordinates (consisting of an affine transformation of the reference image to an active SLO image during eye tracking) recorded by the Spectralis to the initial fixation point at the time the SLO reference image was acquired (SLO image center). Fixation points on the retina are shown as *green dots*. The anatomical fovea center is shown as the *magenta dot* and the SLO image center is shown by the *light blue dot*. A higher magnification of the macula area of fixation is shown in the *inset*. (**E**) Kernel density estimation calculates the probability that fixation occurs at any given point on the retina. The 68% isoline (depicted as the *red contour*) encloses a single area of retina, identifying that there is a single PRL. Fixation instability is calculated as the area of the 68% isoline. In this case, fixation instability measures 0.13 deg^2. N, nasal; T, temporal; S, superior; I, inferior.

Goldmann visual field. Each isopter was assigned a *z*-axis value according to the relative luminous energy of the stimulus (I1e = 1000, I2e = 100, I4e = 10). The visual field volume score was obtained by summing the products of each normalized isopter area and its associated *z*-axis value.

Statistical Analysis

Statistical analysis was performed using STATA Version 14 (College Station, TX, USA). Statistical significance was assumed at $P < 0.05$. Wilcoxon rank sum tests were used to compare median fixation instability and eccentricity for all eyes with ON compared with all normal eyes. In patients with unilateral ON, Wilcoxon signed-rank tests were used to compare fixation instability and eccentricity in affected eyes with their corresponding unaffected eye. The 95% confidence intervals (CIs) for median values were calculated using a binomial method. Ordinary least squares linear regression was used to compare fixation instability and eccentricity measures with logMAR acuity and visual field volume. Receiver operating characteristic (ROC) analysis determined optimal threshold values for detecting ON and central visual field defects (central scotomata), based on fixation instability and fixation eccentricity. Central visual loss was defined as the inability to detect the I2e stimulus within the central 5° on Goldmann perimetry or a reduction in sensitivity in the four center-most stimulus locations on Humphrey automated perimetry by more than 5 dB. Optimal threshold values maximized the sum of sensitivity and specificity for each ROC analysis.

Correlation of Fixation With Retinal GCL Thickness

Three-dimensional automated segmentation of the GCC (GCL + IPL) was reviewed for accuracy, and manual correction of the GCC segmentation was performed if necessary. Ganglion cell complex thickness maps with voxel size 21 × 21 pixels (0.41° × 0.41°) were created from the segmented data and centered on the fovea. The voxel size represented the smallest possible square voxel size without interpolation and was derived from 49 B-scans that cover 20° (20°/49 = 0.41°).

To determine whether a structural–functional relationship exists between fixation and areas of intact GCL, the coordinates of the fixation points on the retina (corresponding to photoreceptors) were transformed to the coordinates of RGC soma within the GCC thickness map by implementing a 2D model to account for displacement of RGC soma from their corresponding photoreceptor inner segments (Fig. 3).[16] Kernel density estimation was applied to the locations of these RGC soma to identify preferred loci overlying the GCC thickness map

Investigative Ophthalmology & Visual Science

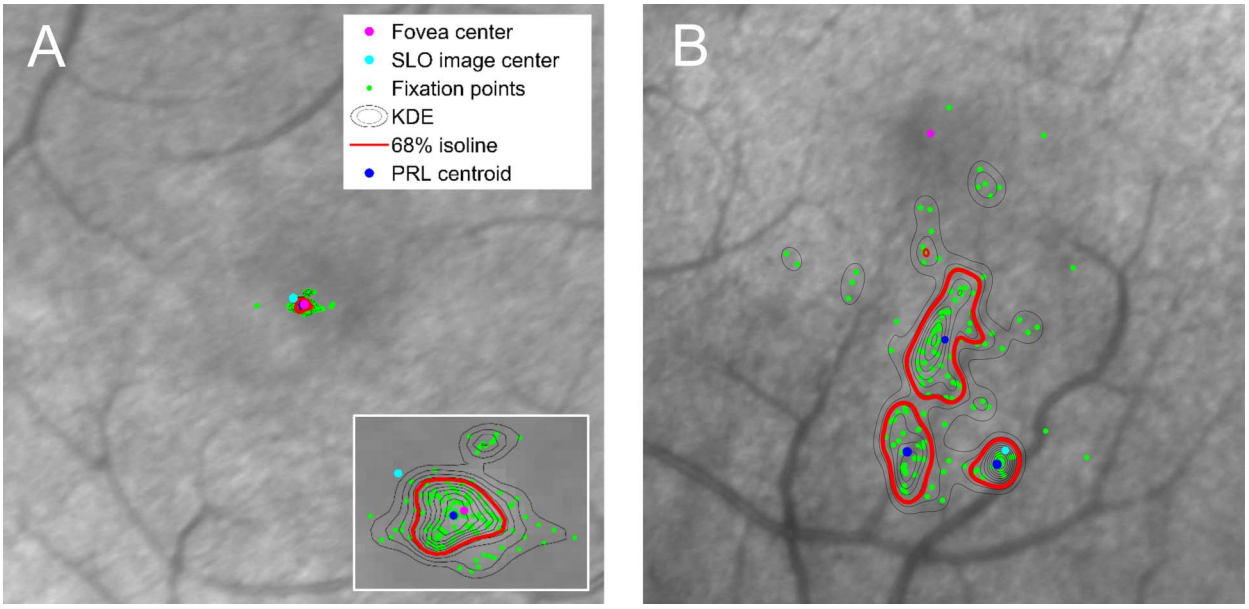

Figure 2. Comparison of fixation in a normal patient and in a patient with optic neuropathy (larger frames are shown at equal magnification). (**A**) In a normal patient, fixation occurs within the foveola. Fixation instability, calculated as the area of the 68% isoline of the KDE, equals 0.022 deg^2. Fixation eccentricity, measured as the distance between the PRL centroid and the fovea center, equals 0.024°. (**B**) A patient with LHON and a centrocecal scotoma has eccentric fixation with three distinct PRLs and fixation instability measuring 1.62 deg^2. When multiple PRLs are identified, a single measure of eccentricity is calculated by taking an average of the distances between the PRL centroids and the fovea center, each weighted according to the number of fixation points within the corresponding PRL. For this patient, fixation eccentricity was 3.26°.

that correlate with the subject's fixation. We termed this area of the GCC thickness map the preferred ganglion cell locus (PGCL).

The PGCL was compared with the GCC thickness map for all eyes with ON and all normal eyes. For unilateral ON eyes where fixation corresponded poorly with remaining GCC thickness, fixation was also compared with the fellow normal eye, and in patients with bilateral ON, fixation was compared with the contralateral affected eye also.

Computational Methods

Computational analysis including image processing, calculation of fixation instability and eccentricity measures, and modeling of ganglion cell displacement from the cone inner segments was performed using custom written code in MATLAB Version 8.5 (MathWorks, Inc., Natick, MA, USA). The Iowa Reference Algorithm used for OCT segmentation was written in the C++ programing language.

Results

Fixation instability (area of the 68% isoline of the KDE) was increased in ON eyes (0.21 deg^2; 95% CI, 0.12–0.32 deg^2) compared with normal eyes (0.069 deg^2; 95% CI, 0.030–0.090 deg^2; $P < 0.001$), as shown in Figure 4A. A paired comparison of the affected eyes with normal eyes of patients with unilateral ON also showed a significant increase in fixation instability in the ON eyes (0.17 deg^2; 95% CI, 0.092–0.37 deg^2) compared with normal eyes (0.063 deg^2; 95% CI, 0.029–0.081 deg^2; $P = 0.001$), as shown in Figure 4B. Similarly, fixation eccentricity was increased in ON eyes (0.48°; 95% CI, 0.25–0.88°) compared with controls (0.24°; 95% CI, 0.17–0.33°; $P = 0.03$), as shown in Figure 4C, and a paired comparison of affected and normal eyes in patients with unilateral ON confirmed an increase in the amount of eccentric fixation in ON eyes (0.58°; 95% CI, 0.23–0.88°) compared with normal eyes (0.24°; 95% CI, 0.17–0.34°; $P = 0.006$) as shown in Figure 4D.

Linear regression analysis (Fig. 5) showed moderate correlation of best-corrected visual acuity expressed as logMAR with fixation instability (adjusted $R^2 = 0.47$; $P < 0.001$) and fixation eccentricity (adjusted $R^2 = 0.49$; $P < 0.001$). Larger values of fixation instability or fixation eccentricity were highly suggestive of the presence of ON and central visual field loss. There was no correlation of visual field volume derived from the Goldmann size I isopters with fixation instability (adjusted $R^2 = 0.04$; $P = 0.15$) or fixation eccentricity (adjusted $R^2 = 0.03$; $P = 0.17$).

Receiver operating characteristic analysis determined the utility of abnormal fixation instability and eccentricity for determining whether a central scotoma was present (Figs. 6A, 6B). The ROC curve for predicting central visual field loss based on fixation instability had an area under the curve (AUC) of 0.93 (Fig. 6A), and the ROC curve for predicting central visual loss based on fixation eccentricity had an AUC of 0.90 (Fig. 6B). A threshold value for fixation instability of greater than 0.25°^{2} had a sensitivity of 79% and specificity of 94%, and a threshold value for fixation eccentricity of greater than 0.8° had a sensitivity of 74% and specificity of 100%.

The ROC curve for predicting ON (with or without a central scotoma) based on fixation instability had an AUC of 0.80, and the ROC curve for predicting ON based on fixation eccentricity had an AUC of 0.68. Optimal sensitivity and specificity values for predicting the presence of ON were calculated for each measure of fixation, giving a sensitivity of 83% and specificity of 68% for fixation instability worse than 0.08 deg^2, and a sensitivity of 57% and specificity of 89% for fixation eccentricity greater than 0.40°.

Twelve of 18 eyes with unilateral ON had PGCLs that were spatially skewed toward the more intact (thicker) areas of the GCC thickness map (Fig. 7A). In patients with bilateral ON (16 eyes), all but 2 eyes had PGCLs that were skewed toward the local maxima of GCC thickness (Fig. 7B). In patients with bilateral, central scotomas with moderate-severely reduced acuities, the PGCL were located in symmetric (homonymous)

Investigative Ophthalmology & Visual Science

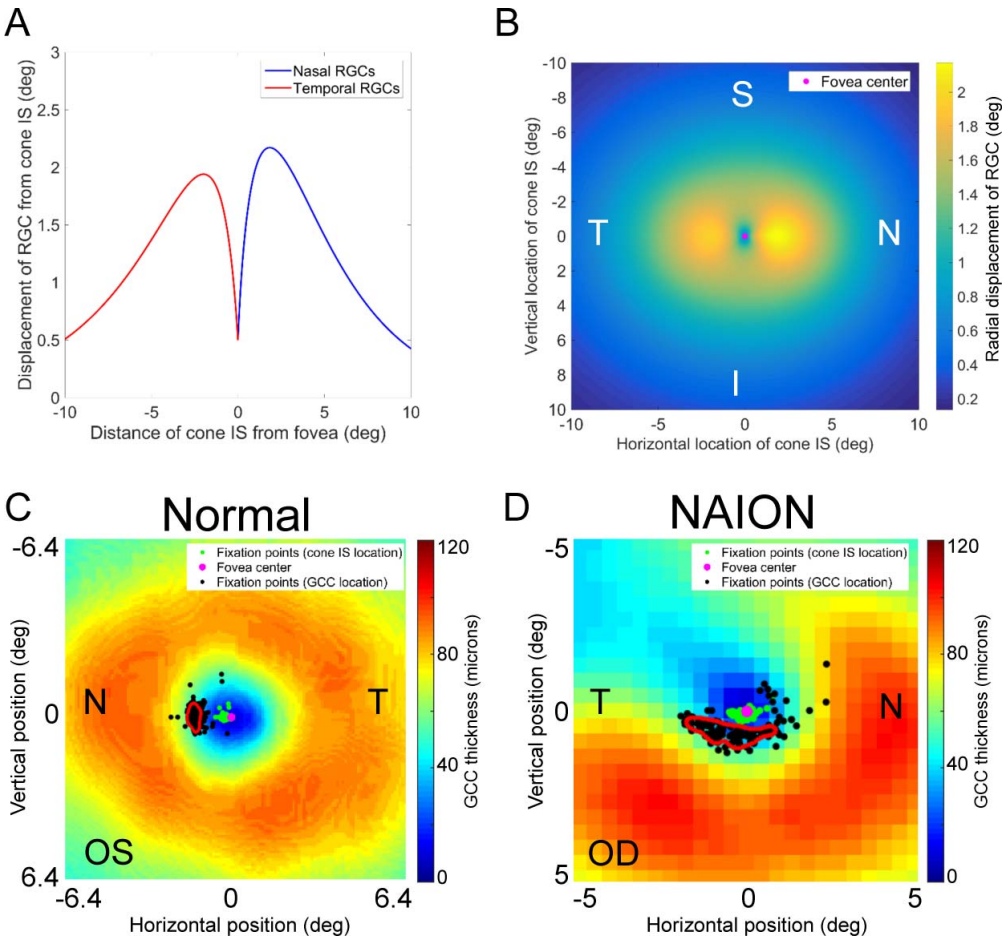

Figure 3. Correlation of retinal GCC thickness with fixation. (**A**) The model by Watson et al. describes the radial displacement of RGC soma from their corresponding cones.[16] The first RGCs are present 150–200 µm from the fovea center, equivalent to approximately 0.5°. Within the central 5° of the fovea center, there is a greater displacement of nasal RGCs compared with temporal RGCs. (**B**) The displacement or RGC soma was generalized to the 2D plane assuming that vertical displacement of RGCs is approximately 75% of horizontal displacement.[18] (**C**) Each fixation point on the retina was taken as the location of a cone and transformed into an RGC location using the transformation map shown in **B**. Kernel density estimation identified a PGCL (outlined by the *red contour*), representing the preferred area of the GCC used for fixation. The fixation pattern of the left eye of a patient without vision loss is shown. The fixation points corresponding to the cone inner segments lie on the slope of the foveal pit, immediately nasal to the fovea center. The ganglion cells corresponding to these cones are displaced radially from the fovea center according to our model. (**D**) In a patient with altitudinal visual field loss due to nonarteritic ischemic optic neuropathy, the PGCL (outlined by the *red contour*), is skewed toward the intact GCC, suggesting a strong correlation between fixation and remaining GCC. N, nasal; T, temporal; S, superior; I, inferior.

regions of the GCC with respect to the fovea (Fig. 7C). In four of six eyes where PGCL corresponded unexpectedly to local minima of the GCC thickness maps, the position of the PGCL relative to the fovea was similar to that of the contralateral unaffected eye (Fig. 7D). In total, 26 of 35 eyes with ON had a pattern of fixation on the retina that correlated spatially with the intact region of the ganglion cell thickness map.

Discussion

The manner by which patients with central visual loss fixate is fundamental to interpreting clinical tests of visual function and represents an important measure for understanding how patients adapt to visual loss. In patients with retinal disease or ON, improvement in visual function measurements are likely due to functional recovery of injured elements of the retina or optic nerve or changes in the receptive field properties of recipient neurons in visual cortex, resulting in adaptive changes in fixation. Disentangling the effects of these distinct processes to better understand the contribution of each is critical for assessing the efficacy of targeted therapies for retinal disease and ONs.

We implemented a method to take advantage of the cSLO-based retinal tracking capabilities of newer generation OCT devices to assess fixation abnormalities and derive the pattern of fixation relative to the GCC in patients with ON. We found that fixation preferences, as quantified by fixation instability and eccentricity measures, were altered in patients with ON. Eyes with ON had a 2- to 3-fold increase in fixation instability and a greater than 2-fold increase in fixation eccentricity compared with normal eyes. As suggested by ROC analysis, fixation instability and eccentricity measures were only moderately predictive of the presence of ON. This was most likely influenced by the fact that, of the ON eyes tested in this study, not all had central visual loss affecting fixation. However, when ROC analysis was performed comparing eyes with central scotomata versus without central scotomata, increased fixation instability and eccentricity were highly predictive of the presence of central visual field loss (Fig. 6). A large proportion of the affected eyes (16/35), such as those with altitudinal visual field loss, had areas of preserved central visual

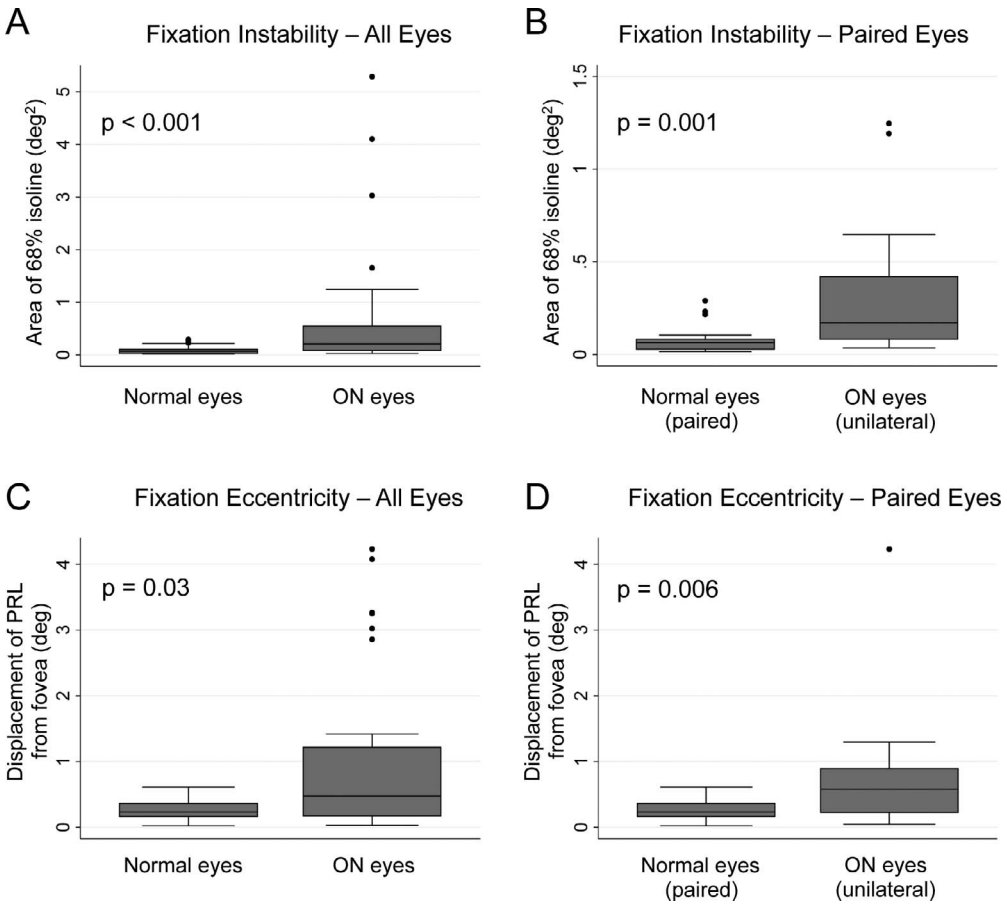

Figure 4. Fixation instability and eccentricity measures for ON eyes and normal eyes. (**A**) Comparison of all eyes with ON and all normal eyes shows that fixation instability is increased in ON eyes ($P < 0.001$). (**B**) A significant difference in fixation instability is still present when performing a paired comparison of affected and unaffected eyes of patients with unilateral ON ($P = 0.001$). Note the different in the *y*-axis scales in (**A**) and (**B**). (**C**) Fixation eccentricity is increased in all ON eyes compared with all normal eyes ($P = 0.03$), and (**D**) a significant difference remains when comparing affected and unaffected eyes with unilateral ON ($P = 0.006$).

field and only moderately affected fixation stability or eccentricity. Another interesting pattern was the presence of a "fenestration" within a central scotoma that allowed a person to centrally fixate, even though a dense scotoma was plotted using standard perimetric testing. This highlights another value of precise assessment of retinal fixation points that may contradict visual acuity measurements recorded using a standard logMAR acuity test; small seeing areas within a large, dense central scotoma may not be apparent by standard visual acuity testing, depending on the size letter that a patient is shown.

Fixation stability and eccentricity measures correlated only moderately with best-corrected logMAR visual acuity, suggesting their utility for providing additive information about central visual function. While visual acuity measurements assess the ability to resolve features of an accommodative target, fixation is a dynamic process that is dependent on the target type and luminance properties, and patients with vision loss may shift fixation between multiple PRLs. The lack of correlation of fixation stability and eccentricity with global measures of visual field volume confirms that fixation is predominantly affected by changes in central visual function.

Measures of fixation are capable of interrogating the function of perifoveal retinal elements in a manner that is beyond the spatial resolution of standard perimetry and may provide additional information not evident on visual field testing. Normal eyes fixated with a mean eccentricity of 0.26° from the fovea anatomical center; the retinal area of fixation did not always colocalize with the nadir of the foveal pit and was often located over the slope of the foveal pit. Optic neuropathy eyes had a median fixation eccentricity of 0.48° from the fovea anatomic center; the closest stimuli to the fixation target in standard clinical automated perimetry is 3° using a 24-2 test strategy and 1° using a 10-2 test strategy and therefore do not provide the spatial resolution needed to precisely assess fixation. Also, with standard perimetry, the location of fixation is not recorded at the time visual threshold is tested, leading to potential errors in the detection and localization of a small scotoma.

The work by others to model the displacement of RGC soma from their corresponding cones[16–18] has provided a framework for relating measures of visual function to structural changes of the GCC in patients with ON.[19–21] Fixation in normal patients occurs within the foveola zone (mean eccentricity from the fovea center of 0.26° in the normal eyes in our study), and the first RGCs do not appear until 150–200 μm (approximately 0.5°) radial from the fovea center. In patients with ON who fixate eccentrically, there can be an up to a 2° difference in the location of the retinal cones with respect to the corresponding RGC soma (Fig. 3A). Correction for RGC displacement is therefore critical for relating the location of fixation on the retina to local areas of the GCC.

Investigative Ophthalmology & Visual Science

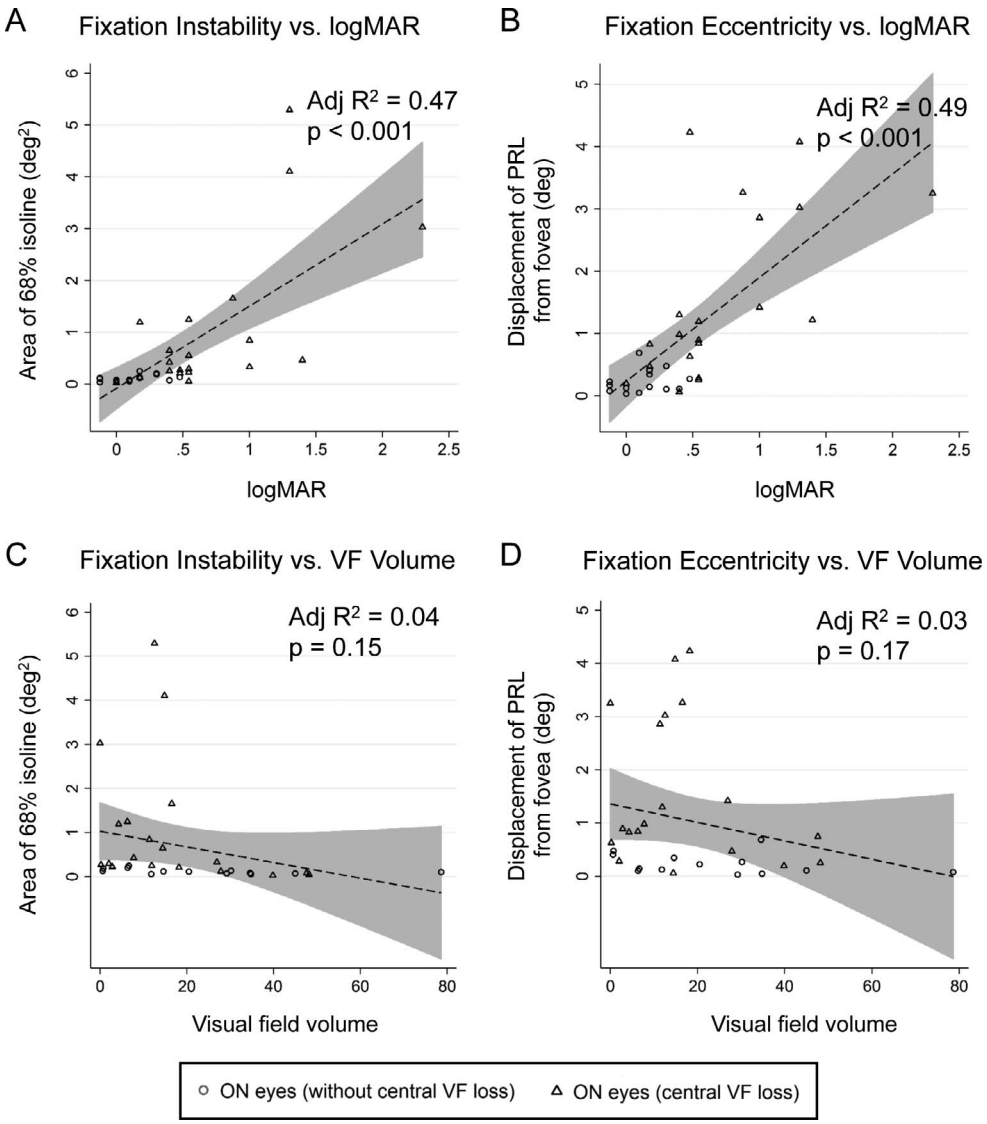

Figure 5. Comparison of fixation instability and fixation eccentricity with logMAR and visual field volume. Linear regression analysis was performed on data for all eyes with ON; 95% prediction limits are shaded *gray*. (**A**) Fixation instability shows moderate correlation with the best-corrected visual acuity expressed as the logMAR (adjusted $R^2 = 0.47$; $P < 0.001$). Eyes with worse logMAR and greater fixation instability tended to have central visual field loss. (**B**) Fixation eccentricity shows moderate correlation with logMAR (adjusted $R^2 = 0.49$; $P < 0.001$). Eyes with worse logMAR and increased fixation eccentricity tended to have central visual field loss. (**C**, **D**) Fixation instability (adjusted $R^2 = 0.04$) and fixation eccentricity (adjusted $R^2 = 0.03$) each showed no correlation to visual field volume calculated from the I1e, I2e, and I4e Goldmann visual field isopters.

Our analysis of fixation based on GCC thickness provided several important observations. Fixation correlated with thicker regions of GCC thickness in a majority of ON eyes, but in some patients, correlated with a relatively thinned region. Poor correlation occurred in six patients with unilateral ON, four of whom had PGCLs that were highly similar to the PGCL of the contralateral normal eye; this suggests that patients with unilateral ON may utilize suboptimal fixation in the affected eye due to the influence from the unaffected, better-seeing eye. Alternatively, PGCLs in relatively thin areas of the GCC may suggest better visual potential than predicted by the degree of GCC thinning. Finally, the pattern of fixation is likely to be task dependent and may be influenced by whether the target is a simple object such as the one used in our study, an optotype, or even words as part of a more complex reading task.[4,5,22–25] The two patients with symmetric bilateral visual loss and central scotomas due to LHON adopted eccentric PRGL located in similar locations in each eye (Fig. 7C). For these patients, the GCC was diffusely thin, and the location of the PRGL may indicate focal areas of better retinal sensitivity or be influenced by optimal placement of the central scotoma to maximize visual function.

In conclusion, retina movement data collected during fixation on an internal target with a cSLO-OCT in patients with ON provides an additional measure of visual function that is highly predictive of central visual loss, influenced primarily by the function of foveal and perifoveal retinal elements, and additive to other clinical testing. We established a framework for relating fixation points on the retina to the GCC thickness map, a tool that will allow further study of the role that fixation plays in improvement of visual function measures after ON. The principle of correlating fixation measured by cSLO-OCT with individual retinal layers is generalizable to patients with other diseases affecting the retina.

Investigative Ophthalmology & Visual Science

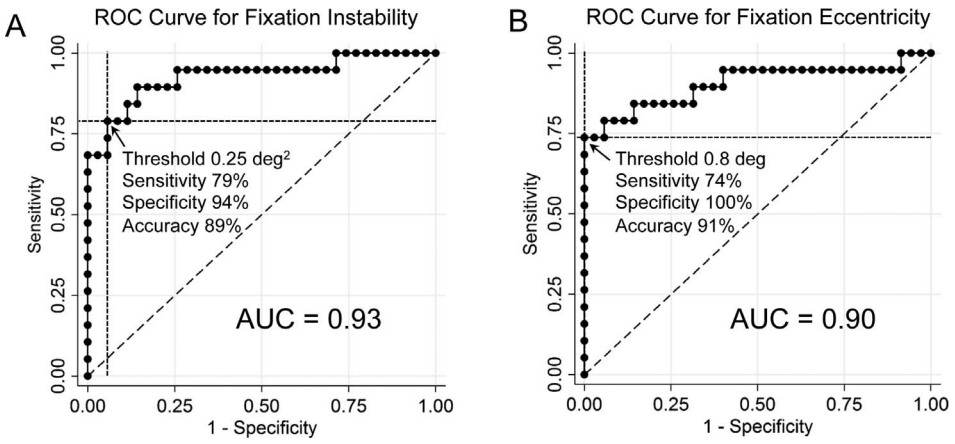

Figure 6. Receiver operating characteristic analysis for fixation instability and eccentricity predicting the presence of a central scotoma. AUC, area under the curve.

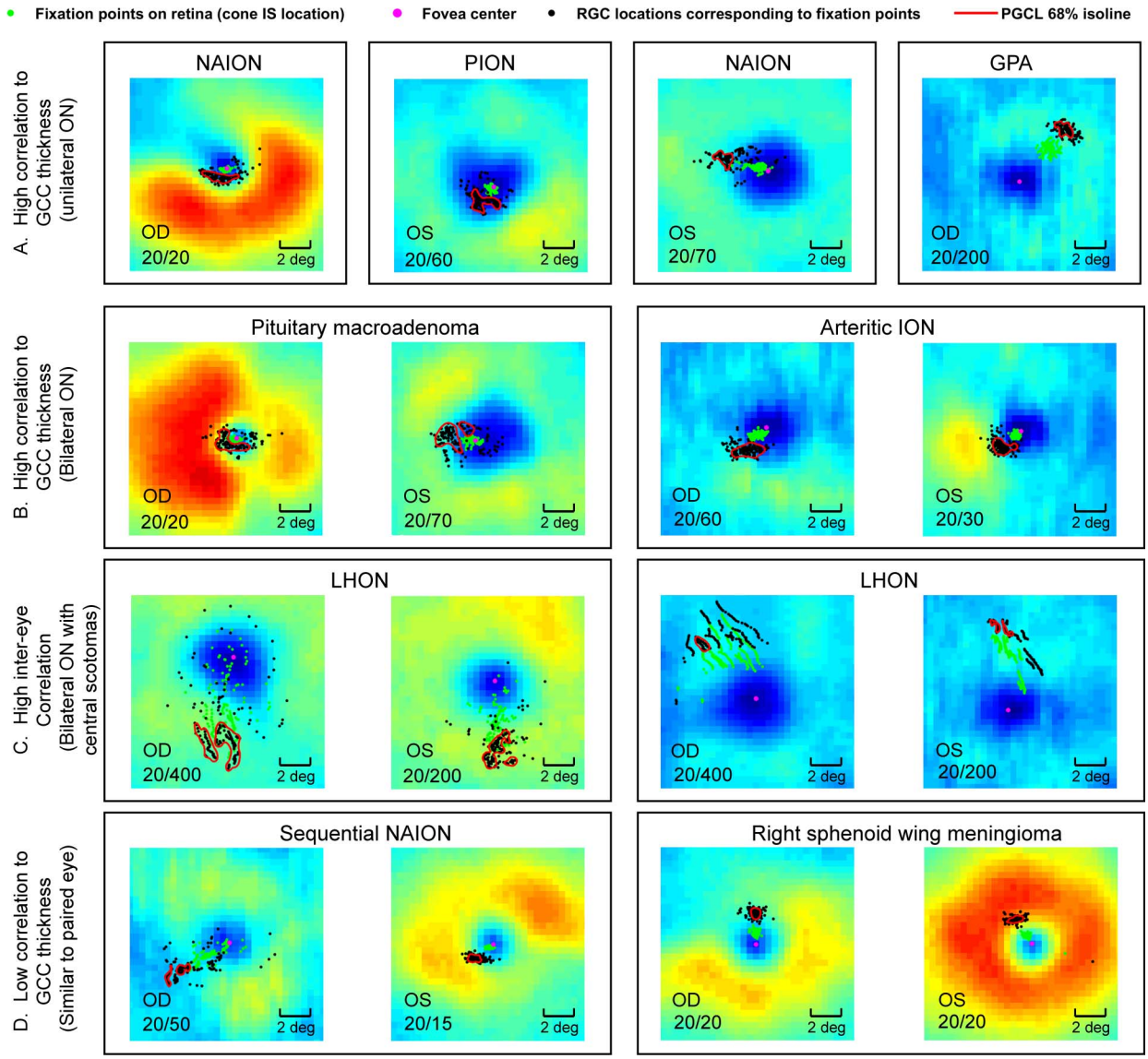

Figure 7. Examples of fixation patterns relative to the GCC thickness map. (**A**) Four ON eyes with PGCL shifted favorably toward the thickest region of the GCC. (**B**) Two patients with bilateral ON and PGCL that correlate highly with the more intact, thicker locations of GCC. (**C**) Two patients with bilateral dense central scotomas and eccentric fixation with PGCL displaced in the same general location from the fovea in the right and left eye of the same patient. (**D**) Two patients with fixation correlating poorly to the GCC in the eye with greater visual field and structural loss. GPA, granulomatosis with polyangiitis; LHON, Leber hereditary optic neuropathy; NAION, nonarteritic anterior ischemic optic neuropathy; PION, posterior ischemic optic neuropathy.

Investigative Ophthalmology & Visual Science

Acknowledgments

The authors thank Jan M. Full, RN, for her technical expertise in acquiring OCT data.

Supported by Iowa City VA Center for the Prevention and Treatment of Visual Loss Grant C9251-C, Rehabilitation Research & Development (RR&D), VA Office of Research and Development; Department of Defense Grant W81XWH-10-1-0736, (Objective Methods to Test Visual Dysfunction in the Presence of Cognitive Impairment); and the Viragh Foundation through collaboration with Elliot Frohman, MD, PhD, and Teresa Frohman, PA (Department of Neurology and Neurotherapeutics, University of Texas Soutwestern Medical Center).

Disclosure: **R.M. Mallery**, None; **P. Poolman**, None; **M.J. Thurtell**, None; **J.-K. Wang**, None; **M.K. Garvin**, None; **J. Ledolter**, None; **R.H. Kardon**, None

References

1. Fletcher DC, Schuchard RA. Preferred retinal loci relationship to macular scotomas in a low-vision population. *Ophthalmology*. 1997;104:632–638.
2. Reinhard J, Messias A, Dietz K, et al. Quantifying fixation in patients with Stargardt disease. *Vision Res*. 2007;47:2076–2085.
3. Kumar G, Chung STL. Characteristics of fixational eye movements in people with macular disease. *Invest Ophthalmol Vis Sci*. 2014;55:5125–5133.
4. Sunness JS, Applegate CA, Haselwood D, Rubin GS. Fixation patterns and reading rates in eyes with central scotomas from advanced atrophic age-related macular degeneration and Stargardt disease. *Ophthalmology*. 1996;103:1458–1466.
5. Sunness JS, Applegate CA. Long-term follow-up of fixation patterns in eyes with central scotomas from geographic atrophy that is associated with age-related macular degeneration. *Am J Ophthalmol*. 2005;140:1085–1093.
6. González EG, Tarita-Nistor L, Mandelcorn ED, Mandelcorn M, Steinbach MJ. Fixation control before and after treatment for neovascular age-related macular degeneration. *Invest Ophthalmol Vis Sci*. 2011;52:4208–4213.
7. Altpeter EK, Blanke BR, Leo-Kottler B, Nguyen XN, Trauzettel-Klosinski S. Evaluation of fixation pattern and reading ability in patients with Leber hereditary optic neuropathy. *J Neuroophthalmol*. 2013;33:344–348.
8. Burton R, Smith ND, Crabb DP. Eye movements and reading in glaucoma: observations on patients with advanced visual field loss. *Graefes Arch Clin Exp Ophthalmol*. 2014;252:1621–1630.
9. Hadavi S, Markowitz SN, Reyes SV. Leber's neuropathy and preferred retinal loci. *Can J Ophthalmol*. 2013;48:e8–e9.
10. Smith ND, Glen FC, Crabb DP. Eye movements during visual search in patients with glaucoma. *BMC Ophthalmol*. 2012;12:45.
11. Lee K, Niemeijer M, Garvin MK, Kwon YH, Sonka M, Abramoff MD. Segmentation of the optic disc in 3-D OCT scans of the optic nerve head. *IEEE Trans Med Imaging*. 2010;29:159–168.
12. Garvin MK, Abramoff MD, Kardon R, Russell SR, Wu X, Sonka M. Intraretinal layer segmentation of macular optical coherence tomography images using optimal 3-D graph search. *IEEE Trans Med Imaging*. 2008;27:1495–1505.
13. Garvin MK, Abràmoff MD, Wu X, Russell SR, Burns TL, Sonka M. Automated 3-D intraretinal layer segmentation of macular spectral-domain optical coherence tomography images. *IEEE Trans Med Imaging*. 2009;28:1436–1447.
14. Wang J-K, Kardon RH, Kupersmith MJ, Garvin MK. Automated quantification of volumetric optic disc swelling in papilledema using spectral-domain optical coherence tomography volumetric quantification of optic disc swelling. *Invest Ophthalmol Vis Sci*. 2012;53:4069–4075.
15. Crossland MD, Sims M, Galbraith RF, Rubin GS. Evaluation of a new quantitative technique to assess the number and extent of preferred retinal loci in macular disease. *Vision Res*. 2004;44:1537–1546.
16. Watson AB. A formula for human retinal ganglion cell receptive field density as a function of visual field location. *J Vis*. 2014;14(7):15.
17. Curcio CA, Allen KA. Topography of ganglion cells in human retina. *J Comp Neurol*. 1990;300:5–25.
18. Drasdo N, Millican CL, Katholi CR, Curcio CA. The length of Henle fibers in the human retina and a model of ganglion receptive field density in the visual field. *Vision Res*. 2007;47:2901–2911.
19. Raza AS, Cho J, de Moraes CGV, et al. Retinal ganglion cell layer thickness and local visual field sensitivity in glaucoma. *Arch Ophthalmol*. 2011;129:1529–1536.
20. Moura AL de A, Raza AS, Lazow MA, De Moraes CG, Hood DC. Retinal ganglion cell and inner plexiform layer thickness measurements in regions of severe visual field sensitivity loss in patients with glaucoma. *Eye*. 2012;26:1188–1193.
21. Raza AS, Zhang X, De Moraes CGV, et al. Improving glaucoma detection using spatially correspondent clusters of damage and by combining standard automated perimetry and optical coherence tomography. *Invest Ophthalmol Vis Sci*. 2014;55:612–624.
22. Lei H, Schuchard RA. Using two preferred retinal loci for different lighting conditions in patients with central scotomas. *Invest Ophthalmol Vis Sci*. 1997;38:1812–1818.
23. Schuchard RA. Preferred retinal loci and macular scotoma characteristics in patients with age-related macular degeneration. *Can J Ophthalmol*. 2005;40:303–312.
24. Déruaz A, Whatham AR, Mermoud C, Safran AB. Reading with multiple preferred retinal loci: implications for training a more efficient reading strategy. *Vision Res*. 2002;42:2947–2957.
25. Thaler L, Schütz AC, Goodale MA, Gegenfurtner KR. What is the best fixation target? The effect of target shape on stability of fixational eye movements. *Vision Res*. 2013;76:31–42.

Investigative Ophthalmology & Visual Science